

## Inhibiting Effects of Ethanethiol, Dimethyl Sulfide, and Dimethyl Disulfide on the Corrosion of Stainless Steel (405) in Sulfuric Acid

Jalal Mohammed SALEH\*,† and Yousif Kadim AL-HAIDARI

Department of Chemistry, College of Science, University of Baghdad, Baghdad, Jadiriya, Republic of Iraq  
(Received February 19, 1988)

The corrosion behavior of stainless steel (405) specimen in 5 M  $\text{H}_2\text{SO}_4$  solution has been investigated potentiostatically at four temperatures in the range 303–323 K. The inhibiting effects of ethanethiol ( $\text{EtSH}$ ), dimethyl sulfide ( $\text{Me}_2\text{S}$ ), and dimethyl disulfide ( $\text{Me}_2\text{S}_2$ ) have thereafter been tested for four inhibitor concentrations of 0.5, 1, 5, and 10  $\text{mmol dm}^{-3}$ . The sulfur compound addition to the  $\text{H}_2\text{SO}_4$  solution caused a shift, mainly in the cathodic direction, of the corrosion potential, the electrode potential at low current densities as well as of the linear section of the cathodic Tafel line. The protection efficiency of each sulfur compound was determined at various temperatures and inhibitor concentrations. The sulfur compound acted as a corrosion inhibitor in the  $\text{H}_2\text{SO}_4$  solution through adsorption on the stainless steel surface. The kinetic results, operating through a compensation effect, could well account for the variation of the inhibiting capacities of the various sulfur compounds. The results indicated that inhibition process involved the shift of the stainless steel corrosion to those surface sites which are associated with progressively higher energy of activation.  $\text{EtSH}$  was the most efficient of the three sulfur compounds for inhibiting the corrosion of the stainless steel in  $\text{H}_2\text{SO}_4$  solution.

There have been a number of corrosion and corrosion inhibition investigations on various types of stainless steel in the acid media.<sup>1–7)</sup> The majority of the previous literature was devoted to the effect of the type of stainless steel on the polarization behavior of this alloy in the corrosion medium, as well as to the ability of organic compounds in general to inhibit the steel corrosion.<sup>8–10)</sup>

Organic sulfur compounds have widely been used as inhibitors for the corrosion of various iron alloys.<sup>11–15)</sup> The literature in this respect discusses some effects of such inhibitors which could result in the corrosion inhibition, and these involved:

- (i) altering the nature of the corrosion product;
- (ii) changing the type and the extent of adsorption of the inhibitor on the electrode surface, and;
- (iii) rearranging the corrosion current and potential.

There are several other aspects of the corrosion inhibition which are still lacking. Among such aspects are the thermodynamics of the feasibility of inhibition and the kinetics of the corrosion in the presence and absence of the inhibitor in the corrosion medium, and these need careful attention and thorough investigation.

The present research involves the potentiostatic study of the corrosion of a stainless steel specimen (type 405) in 5 M  $\text{H}_2\text{SO}_4$  (1 M = 1  $\text{mol dm}^{-3}$ ) at four temperatures in the range 303–323 K. The protection efficiencies of three sulfur compounds have been studied at the four experimental temperatures using four concentrations of the inhibitor over the range 0.5 to 10  $\text{mmol dm}^{-3}$ . An attempt was made to predict the thermodynamic feasibility of inhibition from the coverages of the stainless steel surface by the adsorbed

inhibitor. The effect of the inhibitor on the kinetics of the stainless steel corrosion was also attempted from the rates of corrosion under various experimental conditions.

### Experimental

The stainless steel (405) specimen had the following composition as revealed by emission spectroscopic analysis:

element :	Cr	Al	C	Mn	Si	P	S
Wt% :	11.5	0.1	0.08	1.0	1.0	0.04	0.03

Cylindrical working electrodes were made of 8.5 mm thickness and 12.7 mm diameter. The surface of each electrode was carefully polished and then degreased and washed as described earlier.<sup>16)</sup> A tight fitting Teflon sleeve was fitted over one end of the stainless steel electrode to expose an apparent surface area of about 1.0  $\text{cm}^2$  of the stainless steel. The surface preparation procedure was shown to give reproducible polarization curves, with an error in corrosion current density of less than 0.1%. The surface area of the electrode was determined by measuring all dimensions to the nearest 0.01 mm and subtracting the area under the Teflon gasket. A two-dimensional measuring microscope (Pye 6147 M) was used for area measurements.

The experimental cell which had a working compartment capacity of 750  $\text{cm}^3$  contained the stainless steel electrode and two platinum auxiliary electrodes and a saturated calomel electrode connected through a Luggin capillary bridge. The cell compartment was provided with a stirrer and arrangements for bubbling gases through the cell solution. Before each experiment, the solution was deaerated by bubbling highly pure nitrogen gas for 2 h. The cell solution was prepared from triply distilled water and Analar grade  $\text{H}_2\text{SO}_4$ . Ethanethiol ( $\text{EtSH}$ ), dimethyl sulfide ( $\text{Me}_2\text{S}$ ), and dimethyl disulfide ( $\text{Me}_2\text{S}_2$ ) were purum grades, obtained from Fluka, with a purity exceeding 99.5%.

The potential-current curves were plotted<sup>16)</sup> using 'corrosorpt' obtained from Tacussel électronique, which was composed of a potentiostat, an electronic millivoltmeter and

† Saddam University for Engineering and Science, College of Science, Baghdad, Jadiriya, P.O. Box 47077, Iraq.

a chart recorder. The potentiostat had an output voltage of  $\pm 10$  V, output current of  $\pm 500$  mA and a response time of 2–3  $\mu$ s. The recorder enabled the working electrode current to be recorded in either linear or logarithmic coordinates.

Both the cathodic and anodic current-potential curves were obtained with decreasing and increasing polarization and this was repeated several times. The potential scan began initially 1 h after the specimen immersion in the acid solution, beginning at about  $-1.5$  V and proceeded through to  $1.0$  V versus a saturated calomel electrode. A potentiodynamic potential sweep rate of  $15 \text{ mV min}^{-1}$  was used recording the current continuously with the change of potential.

Corrosion current densities ( $i_{\text{corr}}$ ) and corrosion potentials ( $E_{\text{corr}}$ ) were calculated from the polarization curves. The linear logarithmic sections of the cathodic and anodic Tafel lines were extrapolated to the point of intersection from which both  $i_{\text{corr}}$  and  $E_{\text{corr}}$  were determined.

### Results and Discussion

**Corrosion Potential ( $E_{\text{corr}}$ ).** Table 1 shows the variation of  $E_{\text{corr}}$  for the stainless steel specimen in 5 M  $\text{H}_2\text{SO}_4$  solution with temperature and inhibitor concentration. Values of  $E_{\text{corr}}$  for the stainless steel in the acid solution in the absence of the inhibitor shifted to less negative values with increasing temperature from 303 to 323 K.  $E_{\text{corr}}$  generally shifted to more negative values with increasing inhibitor concentration in the case of  $\text{Me}_2\text{S}$  and  $\text{Me}_2\text{S}_2$  at all the experimental temperatures. A similar behavior was observed with EtSH over the concentration range  $0.5$ – $1.0 \text{ mmol dm}^{-3}$  at 313 and 323 K; at 303 and 308 K the shift of  $E_{\text{corr}}$  with increasing EtSH concentration was towards less negative values. A similar trend was detected with ethane-

thiol at 313 and 323 K over the concentration variation from 5 to  $10 \text{ mmol dm}^{-3}$ .

**Tafel Slope.** The influence of the inhibitor concentration on the current-potential polarization curve for the stainless steel in the  $\text{H}_2\text{SO}_4$  solution may be summarized as:

1. The electrode potential at low current densities shifted considerably relative to the values in the absence of the inhibitor. The shift was generally towards more cathodic direction except in the case of EtSH at 303 and 308 K for all inhibitor concentrations and at 313 and 323 K for  $5$ – $10 \text{ mmol dm}^{-3}$  where the shift was in the anodic direction (Table 1).

2. The linear part of the cathodic Tafel lines shifted parallel with respect to the original line in the absence of the inhibitor. The shift was generally in the cathodic direction (Fig. 1).

3. The Tafel lines generally maintained their linearity and slope at all inhibitor concentrations and temperatures.

The first two effects (1 and 2) indicate that all the three sulfur compounds had significant effects on the hydrogen evolution reaction. The transfer coefficient ( $\beta$ ) which was calculated from the Tafel slope had values close to 0.5 (Table 2) in agreement with the generally accepted values of this parameter.<sup>17,18</sup> This suggests that sulfur compound adsorption in the double layer does not change the mechanism of hydrogen evolution reaction despite its effect on the rate. This probably indicates that the sulfur compounds which have been used as inhibitors in the present work act through adsorption on the stainless steel surface.<sup>10,19,20</sup>

Table 1. Potentials (V) and Currents ( $\text{A cm}^{-2}$ ) for the Corrosion ( $E_{\text{corr}}$ ,  $i_{\text{corr}}$ ) of Stainless Steel in 5 M  $\text{H}_2\text{SO}_4$  at Different Inhibitor Concentrations (C) and Temperatures (T)

T K	C $\text{mmol dm}^{-3}$	EtSH		$\text{Me}_2\text{S}$		$\text{Me}_2\text{S}_2$	
		$-E_{\text{corr}}$	$i_{\text{corr}}$	$-E_{\text{corr}}$	$i_{\text{corr}}$	$-E_{\text{corr}}$	$i_{\text{corr}}$
303	0.0	0.413	$5.35 \times 10^{-3}$	0.413	$5.35 \times 10^{-3}$	0.413	$5.35 \times 10^{-3}$
	0.5	0.402	$2.70 \times 10^{-3}$	0.430	$4.10 \times 10^{-3}$	0.425	$3.20 \times 10^{-3}$
	1.0	0.390	$1.55 \times 10^{-4}$	0.454	$2.98 \times 10^{-3}$	0.434	$1.18 \times 10^{-3}$
	5.0	0.370	$6.26 \times 10^{-5}$	0.448	$2.00 \times 10^{-3}$	0.447	$9.54 \times 10^{-4}$
	10.0	0.366	$3.15 \times 10^{-5}$	0.442	$6.08 \times 10^{-4}$	0.445	$5.93 \times 10^{-4}$
308	0.0	0.410	$8.50 \times 10^{-3}$	0.410	$8.50 \times 10^{-3}$	0.410	$8.50 \times 10^{-3}$
	0.5	0.407	$3.50 \times 10^{-3}$	0.422	$7.50 \times 10^{-3}$	0.416	$6.00 \times 10^{-3}$
	1.0	0.402	$6.50 \times 10^{-4}$	0.439	$6.00 \times 10^{-3}$	0.436	$4.20 \times 10^{-3}$
	5.0	0.390	$1.70 \times 10^{-4}$	0.444	$3.40 \times 10^{-3}$	0.442	$3.00 \times 10^{-3}$
	10.0	0.372	$5.00 \times 10^{-5}$	0.450	$1.40 \times 10^{-3}$	0.446	$1.40 \times 10^{-3}$
313	0.0	0.407	$1.14 \times 10^{-2}$	0.407	$1.14 \times 10^{-2}$	0.407	$1.14 \times 10^{-2}$
	0.5	0.414	$9.20 \times 10^{-3}$	0.415	$1.10 \times 10^{-2}$	0.421	$9.00 \times 10^{-3}$
	1.0	0.428	$6.80 \times 10^{-3}$	0.427	$1.04 \times 10^{-2}$	0.430	$7.50 \times 10^{-3}$
	5.0	0.400	$7.00 \times 10^{-4}$	0.447	$5.16 \times 10^{-3}$	0.443	$5.15 \times 10^{-3}$
	10.0	0.382	$5.70 \times 10^{-5}$	0.418	$2.37 \times 10^{-3}$	0.448	$2.37 \times 10^{-3}$
323	0.0	0.400	$2.95 \times 10^{-2}$	0.400	$2.95 \times 10^{-2}$	0.400	$2.95 \times 10^{-2}$
	0.5	0.419	$2.65 \times 10^{-2}$	0.416	$2.70 \times 10^{-2}$	0.439	$2.30 \times 10^{-2}$
	1.0	0.438	$2.30 \times 10^{-2}$	0.428	$2.55 \times 10^{-2}$	0.460	$1.58 \times 10^{-3}$
	5.0	0.420	$1.75 \times 10^{-2}$	0.438	$1.65 \times 10^{-2}$	0.464	$8.60 \times 10^{-3}$
	10.0	0.392	$6.69 \times 10^{-4}$	0.450	$7.75 \times 10^{-3}$	0.466	$8.15 \times 10^{-3}$

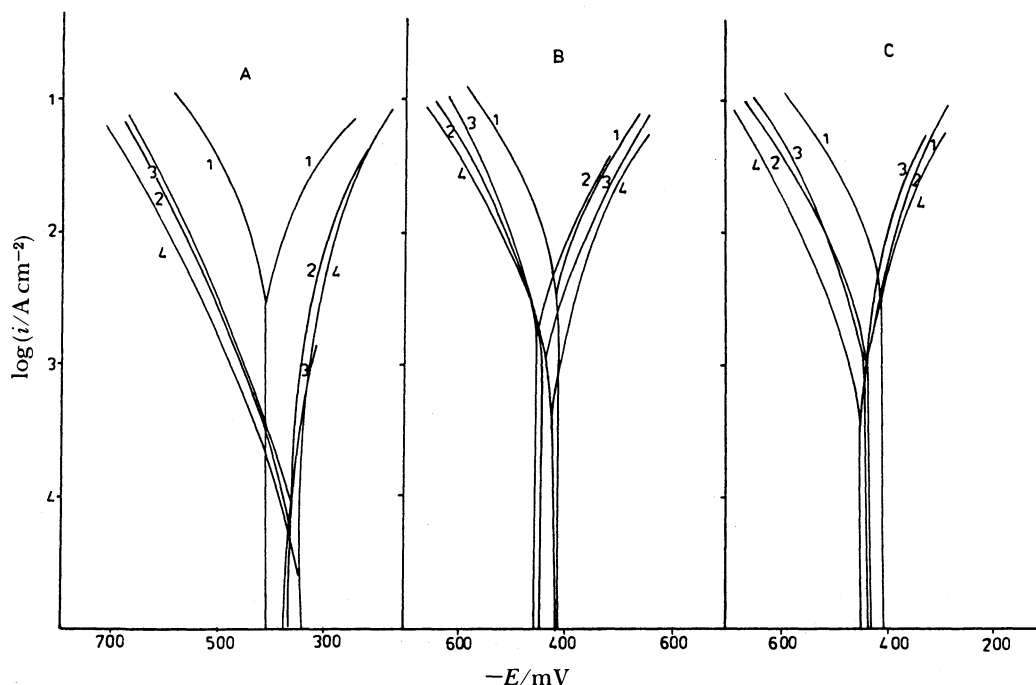


Fig. 1. Effect of the inhibitor on the cathodic and anodic polarization curves for the stainless steel (405) in 5 M  $\text{H}_2\text{SO}_4$  at 303 K. Numbers 1, 2, 3, and 4 refer respectively to the inhibitor concentrations of zero, 1, 5, and 10  $\text{mmol dm}^{-3}$ . A, EtSH; B,  $\text{Me}_2\text{S}$ ; C,  $\text{Me}_2\text{S}_2$ .

Table 2. Effect of Inhibitor Concentration and Temperature on the Surface Coverage ( $\theta$ ), Tafel Slope ( $\beta$ ) and Polarization Resistance ( $R_p$ ) for the Stainless Steel Specimen in 5 M  $\text{H}_2\text{SO}_4$

$T$ K	$C$ $\text{mmol dm}^{-3}$	EtSH			$\text{Me}_2\text{S}$			$\text{Me}_2\text{S}_2$		
		$\theta$	$\beta$	$R_p^a$	$\theta$	$\beta$	$R_p^a$	$\theta$	$\beta$	$R_p^a$
303	0.0	—	0.44	1.68	—	0.44	1.68	—	0.44	1.68
	0.5	0.74	0.45	37.4	0.15	0.45	2.20	0.36	0.43	5.7
	1.0	0.80	0.47	98.9	0.23	0.46	3.27	0.50	0.42	10.2
	5.0	0.82	0.47	163.4	0.51	0.37	3.74	0.73	0.42	8.4
	10.0	0.91	0.46	440.9	0.62	0.43	17.60	0.76	0.49	13.4
313	0.0	—	0.37	1.5	—	0.37	1.53	—	0.37	1.53
	0.5	0.38	0.39	2.3	0.11	0.36	1.40	0.21	0.42	1.55
	1.0	0.47	0.40	2.9	0.17	0.36	1.81	0.30	0.50	1.67
	5.0	0.87	0.41	56.1	0.45	0.40	2.82	0.60	0.49	4.35
	10.0	0.92	0.42	180.4	0.58	0.46	14.5	0.68	0.51	7.35
323	0.0	—	0.63	0.43	—	0.63	0.43	—	0.63	0.43
	0.5	0.16	0.60	0.60	0.11	0.60	0.44	0.10	0.51	0.95
	1.0	0.29	0.58	0.62	0.13	0.61	0.46	0.18	0.45	1.24
	5.0	0.54	0.56	1.01	0.40	0.58	0.86	0.48	0.45	2.02
	10.0	0.62	0.59	22.52	0.55	0.40	2.16	0.62	0.47	1.91

a)  $R_p$  is expressed in  $\text{cm}^{-2}$ .

**Polarization Resistance.** The polarization resistance ( $R_p$ ) may be taken as a measure of the efficiency of the sulfur compounds to operate as corrosion inhibitors for the stainless steel in the  $\text{H}_2\text{SO}_4$  solution, where

$$R_p = d(E - E_{\text{corr}})/di \quad (1)$$

where  $E$  and  $E_{\text{corr}}$  are in V,  $i$  in  $\text{A cm}^{-2}$ , and  $R_p$  in  $\Omega \text{cm}^{-2}$ . For small polarization, values of  $(E - E_{\text{corr}})$  are proportional to the current density  $i$ . Such a relationship was found in the present work to exist for the low cathodic polarization region where  $(E - E_{\text{corr}}) < 20$  mV.

This is an indication for the fact that some stage in the discharge of hydrogen ions at the electrode should be the rate-determining process. Figure 2 shows the relationship between such small  $(E - E_{\text{corr}})$  values and the corresponding values of  $i$ , for the polarization in the absence and the presence of the inhibitors. Values of  $R_p$  have been derived from the slopes of various plots in Fig. 2 and these are presented in Table 2.

**Protection Efficiency.** The protection efficiency ( $P$ ) of the sulfur compounds, operating as inhibitors, could be calculated from equation:<sup>15,16,21)</sup>

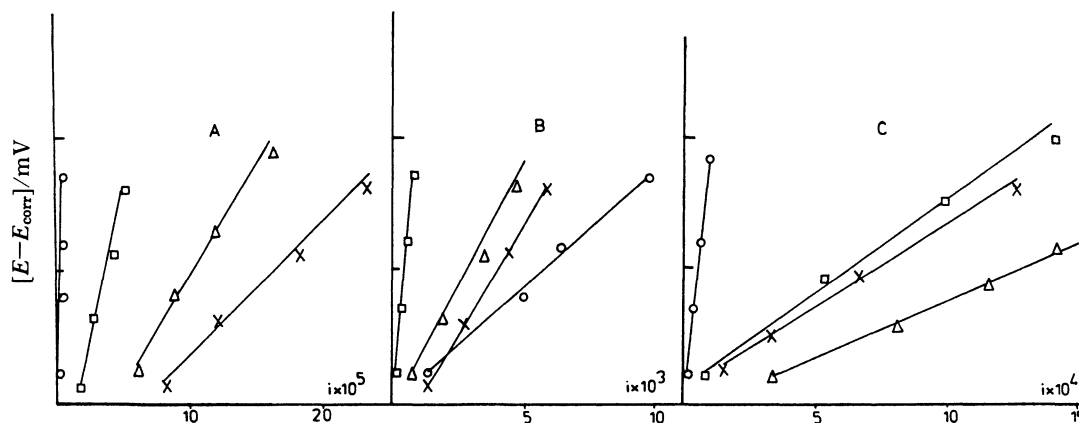


Fig. 2. Values of  $(E - E_{\text{corr}})$  plotted against the current density ( $i$ ) for low cathodic polarization of the stainless steel (405) in 5 M  $\text{H}_2\text{SO}_4$  at 303 K. Symbols O, X, Δ, and □ refer respectively to inhibitor concentrations of zero, 1, 5, and 10  $\text{mmol dm}^{-3}$ . Other symbols (A, B, and C) as in Fig. 1.

Table 3. Effect of Inhibitor Concentration ( $C$ ) at Three Temperatures on the Values of the Protection Efficiency ( $P$ ) of the Various Inhibitors in the 5 M  $\text{H}_2\text{SO}_4$  Solution of the Stainless Steel Specimen

$C$ $\text{mmol dm}^{-3}$	$P$								
	303 K			313 K			323 K		
	EtSH	$\text{Me}_2\text{S}$	$\text{Me}_2\text{S}_2$	EtSH	$\text{Me}_2\text{S}$	$\text{Me}_2\text{S}_2$	EtSH	$\text{Me}_2\text{S}$	$\text{Me}_2\text{S}_2$
0.5	54.7	23.4	40.2	19.3	4.5	19.0	10.2	8.5	21.1
1.0	97.1	44.3	77.9	40.6	8.0	34.1	22.0	13.6	46.4
5.0	98.8	62.6	82.2	99.3	40.6	54.7	40.7	44.1	70.8
10.0	99.4	88.7	88.9	99.5	79.2	79.1	97.3	73.7	72.4

$$P = 100[1 - (i_c)_2 / (i_c)_1] \quad (2)$$

where  $(i_c)_1$  and  $(i_c)_2$  are respectively the corrosion current densities ( $i_{\text{corr}}$ ) for the stainless steel in the absence and the presence of the sulfur compound in the acid solution at the same temperatures;  $(i_c)_1$  and  $(i_c)_2$  are assumed to be proportional respectively to the corrosion rates under similar experimental conditions in the absence and the presence of the inhibitor in the corrosion medium.<sup>22)</sup> Values of  $P$  that have been calculated, for the three sulfur compounds, from the data of Table 1 are indicated in Table 3.

Values of  $P$  generally increased at all the experimental temperatures with increasing concentration of the inhibitor (Table 3). The highest protection efficiency ( $P_h$ ) of the sulfur compounds was attained at 303 K, as well as at 313 K in the case of EtSH, and corresponded to inhibitor concentration of 10  $\text{mmol dm}^{-3}$ .  $P_h$  values of the three sulfur compounds could be arranged in the order:  $\text{EtSH} > \text{Me}_2\text{S}_2 > \text{Me}_2\text{S}$ . Values of  $P$  at 303 K remained relatively high for EtSH even at 1  $\text{mmol dm}^{-3}$  and the values of  $P$  for this inhibitor at this temperature showed the least dependence on the inhibitor concentration. The least dependencies on the inhibitor concentration were observed with EtSH and  $\text{Me}_2\text{S}$  at 313 and 323 K. At 10  $\text{mmol dm}^{-3}$  of either  $\text{Me}_2\text{S}$  and  $\text{Me}_2\text{S}_2$  in the acid solution,  $P$  became higher at 313 K than the values at 323 K in contrast to the

behavior at 1 and 5  $\text{mmol dm}^{-3}$ . Values of  $P$  decreased only slightly in the case of EtSH at 10  $\text{mmol dm}^{-3}$ , while the decrease of  $P$  for this inhibitor was sharp and substantial at 1 and 5  $\text{mmol dm}^{-3}$  beginning at 303 K in the former case and at 313 K at the latter inhibitor concentration. The decrease of  $P$  with temperature for  $\text{Me}_2\text{S}$  and  $\text{Me}_2\text{S}_2$  was gradual at 10  $\text{mmol dm}^{-3}$ , but the decrease at the other inhibitor concentrations was rather sharp over the range 303–313 K increasing thereafter on raising the temperature to 323 K (Table 3).

**Inhibitor Adsorption.** The coverage ( $\theta$ ) of the stainless steel surface by the adsorbed inhibitor was estimated from the current densities at constant potential in the presence ( $i_2$ ) and absence ( $i_1$ ) of the inhibitor in the acid solution using the equation:<sup>15,23)</sup>

$$\theta = 1 - (i_2 / i_1) \quad (3)$$

Table 2 gives the calculated values of  $\theta$  for the various inhibitors at different experimental temperatures and inhibitor concentrations. At any experimental temperature,  $\theta$  increased with increasing inhibitor concentration. On the other hand, values of  $\theta$ , at a given inhibitor concentration, decreased with the rise of the temperature from 303 to 323 K.

The manner in which the values of  $\theta$  for each inhibitor varied at a constant temperature with the concentration ( $C$ ) of the inhibitor conformed to Langmuir

adsorption isotherm which may be put as:

$$\frac{C}{\theta} = \frac{1}{b} + C \quad (4)$$

A plot of  $C/\theta$  values against the corresponding values of  $C$  was found to be linear with respect to each inhibitor as seen in Fig. 3. The values of  $b$  for each sulfur compound could be estimated from the reciprocal of the intercept of the appropriate plot in Fig. 3. Table 4 gives values of  $b$  for the various sulfur compounds which have been utilized as inhibitors for the corrosion of the stainless steel in the  $\text{H}_2\text{SO}_4$  solution.

The parameter  $b$  in Eq. 4 may be defined as:<sup>24,26)</sup>

$$b = a \exp(-\Delta H_a/RT) \quad (5)$$

where  $\Delta H_a$  is the heat of inhibitor adsorption on the stainless steel surface and  $a$  is a constant.<sup>24)</sup> A plot of  $\log b$  versus  $1/T$  for each sulfur compound should result in a straight line if  $a$  and  $\Delta H_a$  remained constant over the experimental temperature range as was found with the present results indicated in Fig. 4. Values of  $\Delta H_a$  for the temperature range 303–323 K have been derived for the various inhibitors from the slopes of the

plots in Fig. 4 and these have been listed in Table 4. Values of  $\Delta H_a$  are shown (Table 4) to be all negative reflecting the exothermic behavior of the inhibitor adsorption on the stainless steel surface. The magnitude of  $\Delta H_a$  is less negative in the case of  $\text{Me}_2\text{S}$  as compared with the remaining two sulfur compounds. This is an indication for the stronger inhibitor adsorption in the case of  $\text{EtSH}$  and  $\text{Me}_2\text{S}_2$  as compared with that of  $\text{Me}_2\text{S}$ . This result well agrees with that presented in Table 3 for the variation of the protection efficiency of the inhibitors with concentration; values of  $P$  are shown in Table 3 to be generally higher for  $\text{EtSH}$  and  $\text{Me}_2\text{S}_2$  at all inhibitor concentrations than of  $\text{Me}_2\text{S}$ .

The parameter  $b$ , given in Eq. 4 represents the equilibrium constant for the adsorption/desorption processes of the inhibitor on the stainless steel surface and could be expressed as;<sup>24)</sup>

$$b = \exp(-\Delta G_a/RT) = \exp(\Delta S_a/R) \exp(-\Delta H_a/RT) \quad (6)$$

where  $\Delta G_a$ ,  $\Delta S_a$ , and  $\Delta H_a$  are respectively the changes in the free energy, entropy, and enthalpy of the inhibitor adsorption on the stainless steel surface. Values of

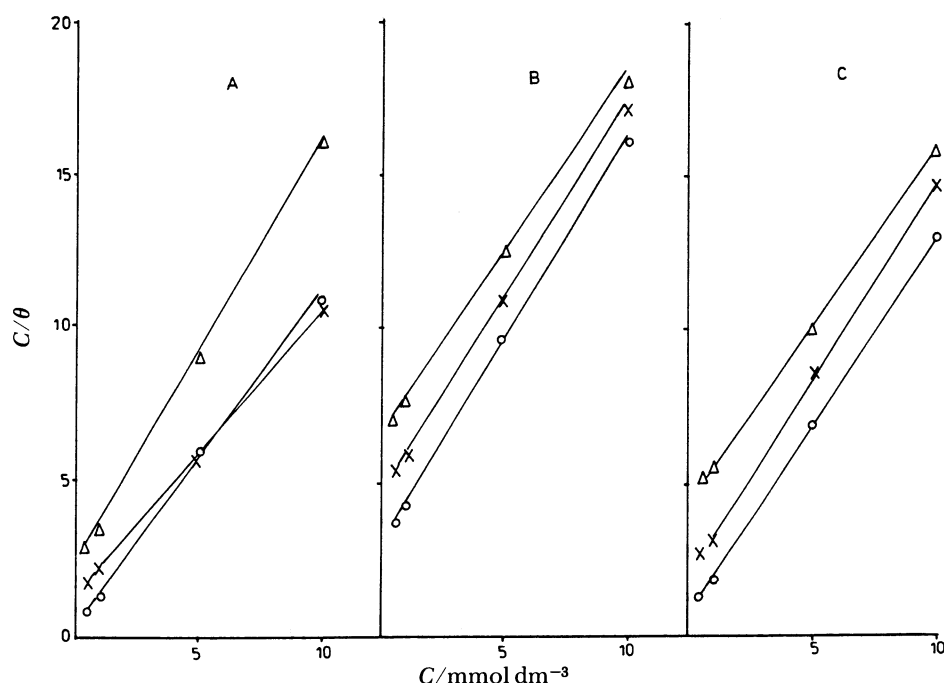


Fig. 3. Langmuir adsorption isotherms plotted as  $C/\theta$  versus  $C$  for the three inhibitors at 303 (○), 313 (×), and 323 K (Δ).

Table 4. Values of  $b$ ,  $\Delta G_a$  ( $\text{kJ mol}^{-1}$ ),  $\Delta H_a$  ( $\text{kJ mol}^{-1}$ ), and  $\Delta S_a$  ( $\text{J K}^{-1} \text{mol}^{-1}$ ) for the Adsorption of the Inhibitors on the Stainless Steel Specimen at Three Temperatures, in the Range 303–323 K

$T$ K	EtSH				Me <sub>2</sub> S				Me <sub>2</sub> S <sub>2</sub>			
	$b$	$-\Delta H_a$	$-\Delta G_a$	$-\Delta S_a$	$b$	$-\Delta H_a$	$-\Delta G_a$	$-\Delta S_a$	$b$	$-\Delta H_a$	$-\Delta G_a$	$-\Delta S_a$
303	2857		20	184	328		14.6	153	1432		18.3	185
313	1053	76.9	18	184	213	31.7	14.0	146	491	74.3	16.0	186
323	433		16	184	151		13.5	140	231		14.7	185

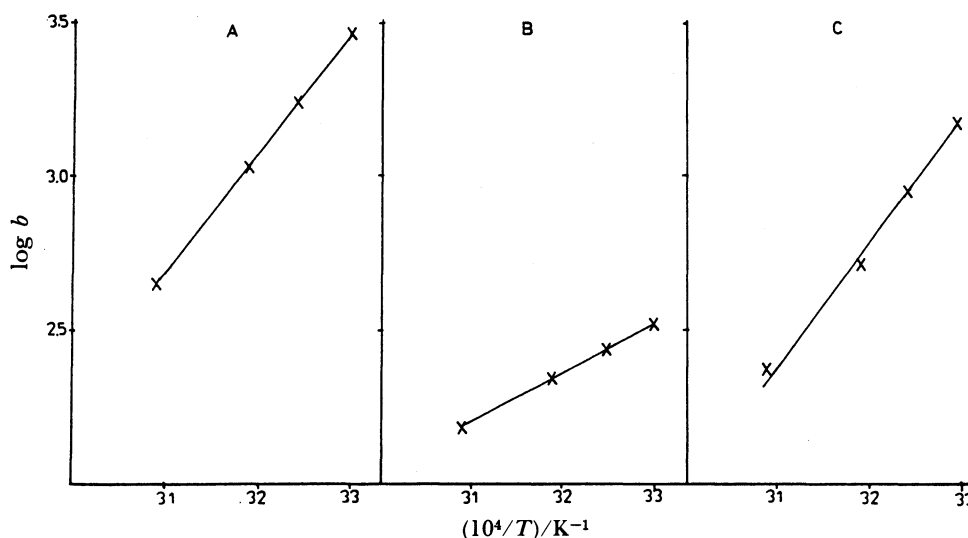


Fig. 4. Values of  $\log b$  plotted versus  $1/T$  for the three inhibitors in the stainless steel/sulfuric acid system.

$\Delta H_a$  have previously been derived from the plots of Fig. 4 which have been presented in Table 4. Using values of  $b$  and  $\Delta H_a$  from Table 4 at each of the four experimental temperatures in the range 303–323 K, it was possible to deduce the corresponding values of  $\Delta G_a$  and  $\Delta S_a$  and these have been inserted in Table 4. Values of  $\Delta G_a$  indicate inhibition of the stainless steel corrosion in the  $H_2SO_4$  solution by the sulfur compounds became less favorable as the temperature increased from 303 to 323 K. This conclusion generally agrees with the results of Table 3 where the values of  $P$  were higher at 303 K than at the higher temperatures. The overall changes in  $\Delta G_a$  and  $\Delta S_a$  over the temperature range 303–323 K are shown in Table 4 to be almost the same for both EtSH and  $Me_2S_2$  and the values are more negative than for  $Me_2S$ . The less negative values of  $\Delta S_a$  for  $Me_2S$  than for EtSH and  $Me_2S_2$  should reflect a far less decrease in the degrees of freedom subsequent to adsorption on the electrode surface in the case of the former inhibitor than of the latter two sulfur compounds. This suggests a weaker adsorbed species as a consequence of  $Me_2S$  adsorption on the stainless steel than those resulting throughout adsorption of EtSH or  $Me_2S_2$ .

**Kinetics of Corrosion.** The rate ( $r$ ) of the stainless steel corrosion in the  $H_2SO_4$  solution increased generally with the rise of the temperature from 303 to 323 K, and the behavior followed Arrhenius equation:

$$r = A \exp(-E/RT) \quad (7)$$

where  $A$  and  $E$  are respectively the preexponential factor and the energy of activation. Due to the linearity of the Tafel slope segment of the current-potential polarization curve, the value of  $r$  in Eq. 7 was taken to be directly proportional to the corrosion current density ( $i_{corr}$ ) through such relation as:<sup>21)</sup>

$$r = 0.13(\theta/d)i_{corr} \quad (8)$$

where  $\theta$  is the equivalent weight of the metal and  $d$  its density. Using the appropriate conversion factor, the values of  $i_{corr}$  at each temperature could be converted into rate ( $i$ ) in units of 'atom  $cm^{-2} s^{-1}$ '. Figure 5 shows Arrhenius plots for the blank (absence of inhibitor) and various inhibitor concentrations; values of  $E$  and  $A$  have been derived from the slopes and intercepts of the plots respectively. Table 5 gives the resulting values of  $E$  and  $\log A$  for the corrosion of the stainless steel specimen in the acid solution. Both  $\log A$  and  $E$  increased smoothly with increasing inhibitor concentration.

A linear relationship was found to exist between the experimental values of  $\log A$  and the corresponding values of  $E$  which could be expressed as:<sup>27)</sup>

$$\log A = mE + l \quad (9)$$

where  $m$  and  $l$  are respectively the slope and the intercept of the plot in Fig. 6. Such a relationship is termed a 'compensation effect' which is frequently found to describe the kinetics of catalytic and a number of tarnishing reactions on metals.<sup>28–31)</sup> Equation 9 shows that simultaneous increases or decreases in  $E$  and  $\log A$  for a particular system tend to compensate from the standpoint of the reaction rate. A number of interpretations have been offered for the phenomenon of the compensation effect in surface reactions,<sup>32–35)</sup> among which the effect could be ascribed to the presence of energetically heterogeneous reaction sites on the metal surface; and the corrosion reaction should therefore occur first on surface sites with low energy of activation and spreading thereafter to those sites where  $E$  values are progressively higher.

The activation energy ( $E$ ) of the stainless steel corrosion in the  $H_2SO_4$  solution in the absence of the inhibitor was 69.5  $kJ mol^{-1}$ ; the corrosion should thus be confined to surface sites with such energy of activa-

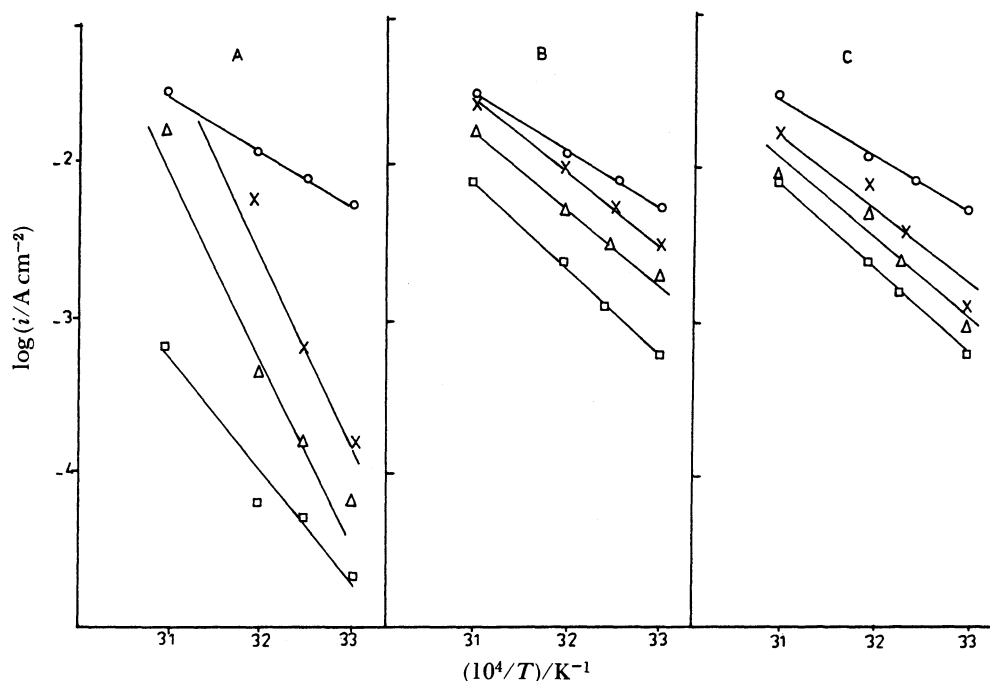


Fig. 5. Arrhenius plots, relating  $\log i_{\text{corr}}$  to  $1/T$ , for the corrosion of the stainless steel (405) in 5 M  $\text{H}_2\text{SO}_4$  in the absence and the presence of the inhibitors in the acid. Symbols as in Fig. 2.

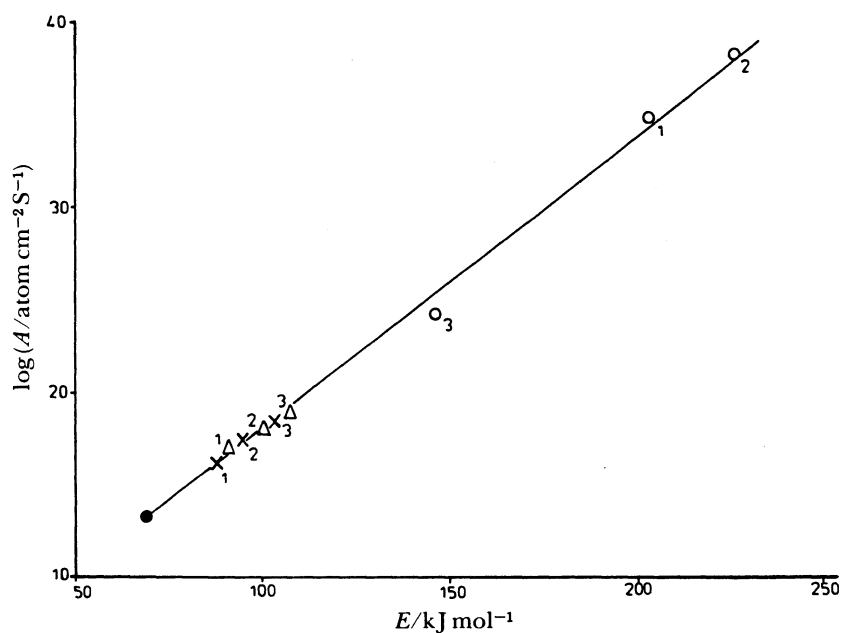


Fig. 6. Variation of the activation energy ( $E$ ) with the preexponential factor ( $\log A$ ) for the corrosion of the stainless steel (405) in 5 M  $\text{H}_2\text{SO}_4$ . EtSH,  $\circ$ ;  $\text{Me}_2\text{S}$ ,  $\Delta$ ;  $\text{Me}_2\text{S}_2$ ,  $\times$ . Numbers 1, 2, and 3 refer respectively to inhibitor concentrations of 1, 5, and 10  $\text{mmol dm}^{-3}$ .  $\bullet$ , corresponds to the value in the absence of the inhibitor.

tion. The presence of the sulfur compound in the acid solution accordingly shifts the corrosion reaction to those sites where  $E$  values are greater. The corrosion reaction will further be pushed to surface sites which are characterized with progressively higher values of  $E$  as the concentration of the inhibitor in the acid solu-

tion became greater.

The results of Fig. 6 and Table 5 reveal the following:

1. For all inhibitor concentrations in the acid, the variation of  $E$  values for the three sulfur compounds, followed the sequence:

Table 5. Activation Energies ( $E$ ) and Preexponential Factors ( $A/\text{atom cm}^{-2} \text{ s}^{-1}$ ) for the Corrosion of the Stainless Steel Specimen in 5 M  $\text{H}_2\text{SO}_4$  at Four Inhibitor Concentrations ( $C$ )

Inhibitor	$C$ $\text{mmol dm}^{-3}$	$\log A$	$E$ $\text{kJ mol}^{-1}$
EtSH	0.0	11.6	69.5
	0.5	32.2	186.5
	1.0	34.7	204.7
	5.0	38.0	227.2
	10.0	24.1	147.0
$\text{Me}_2\text{S}$	0.0	11.6	69.5
	0.5	14.8	78.0
	1.0	16.1	87.7
	5.0	16.8	93.6
	10.0	18.2	103.8
$\text{Me}_2\text{S}_2$	0.0	11.6	69.5
	0.5	15.4	86.5
	1.0	16.8	91.9
	5.0	17.8	100.5
	10.0	18.7	106.8



This reflects the greatest tendency of the stainless steel for corrosion in the acid solution containing  $\text{Me}_2\text{S}$  as compared with the behavior of the specimen in the presence of EtSH under similar inhibitor concentration and temperature. This conclusion agrees with the protection efficiency results which have been presented in Table 3. The results are also in line with the variation of the  $\Delta G_a$  values (Table 4) which have been obtained for the inhibitor adsorption on the stainless steel electrode.

2. The dependence of the  $E$  and  $\log A$  values on the inhibitor concentration is seen in Fig. 6 to be far more smaller in the case of  $\text{Me}_2\text{S}$  and  $\text{Me}_2\text{S}_2$  as compared with that of EtSH.

**Molecular Structure Consideration.** The tendencies of the sulfur compounds to adsorb on, and hence protect, the stainless steel surface are shown from the kinetic results to decrease from EtSH, through  $\text{Me}_2\text{S}_2$ , to  $\text{Me}_2\text{S}$ . A qualitative explanation of this sequence may be found from the consideration of the electronic structures of these compounds. Each of EtSH and  $\text{Me}_2\text{S}$  has one lone pair of electrons on sulfur while there are two such pairs in  $\text{Me}_2\text{S}_2$ . The lone pairs of electrons on the sulfur atoms are delocalized and hence produce delocalization or resonance energy which stabilizes the sulfur compound.<sup>36)</sup> Thus the larger the number of delocalized electrons, the more stable is the charge density on the 'anchoring' atoms (in this case the sulfur) and hence the larger is the strength of adsorption on the metal surface. Comparing  $\text{Me}_2\text{S}_2$  with  $\text{Me}_2\text{S}$ , one would expect stronger adsorption of the former, and therefore greater inhibition, than of the latter. Furthermore, both  $\text{Me}_2\text{S}_2$  and  $\text{Me}_2\text{S}$  do not contain hydrogen atoms linked to sulfur as in the case of EtSH. This should produce an additional adsorp-

tion tendency for this compound (EtSH) on the electrode surface as compared with the remaining two sulfur compounds.

The organic sulfur compounds which have been dealt with in the present work are classified as toxic substances and can inhibit the catalytic activity of metal surfaces due to the presence of lone pairs of electrons on the sulfur atoms.<sup>37)</sup> The poisoning effect results from the formation of strong dative bonds between the toxic molecules and the surface atoms. It has been established that the poisoning effect among a series of alkyl sulfides and disulfides increased by lengthening the chain in these compounds.<sup>38)</sup> These facts showed that  $\text{Me}_2\text{S}_2$  was more toxic than  $\text{Me}_2\text{S}$  and that EtSH behavior was comparable with that of  $\text{Me}_2\text{S}_2$ . This conclusion well agrees with the calculated values of  $\Delta H_a$  (Table 4) as the heat of adsorption is known to be a good measure of the strength of adsorption on a surface.

## References

- 1) T. Ishikawa and G. Okamoto, 1st Intr. Congr. Metal Corrosion, 10—15 April, 1961, Butterworths, London (1961), p. 444.
- 2) I. G. Mugulescu and O. Radevici, 1st Intr. Congr. Metal Corrosion, 10—15 April, 1961, Butterworths, London (1961), p. 302.
- 3) W. O. Binder, J. Thomson, and C. R. Bishop, *Proc. Am. Soc. Test. Mater.*, **56**, 903 (1956).
- 4) M. A. Streicher, *Corrosion*, **14**, 19 (1958).
- 5) D. Warren, *Corrosion*, **16**, 101 (1960).
- 6) V. A. Suprunov and M. Kh. Fried, *Khim-Tekhnol. Inst.*, **12**, 180 (1970) (Russ.).
- 7) J. E. Truman, "Corrosion; Metal/Environment," ed by L. L. Shreir, Newness, Butterworths, Boston, Mass. (1976), Vol. 1, p. 352.
- 8) M. B. Lawson, *Corrosion*, **36**, 493 (1980).
- 9) B. Danmelly, T. C. Downie, and R. Grzeskowiak, *Corros. Sci.*, **14**, 597 (1974).
- 10) H. Brandt, M. Fischer, and K. Schwabe, *Corros. Sci.*, **10**, 631 (1970).
- 11) G. Trabanelli, F. Zucchi, G. Gullini, and V. Carassiti, *Werkst. Korros.*, **20**, 1012 (1969).
- 12) K. Schwabe, G. Reinhard, M. Fischer, and K. Schaarschmidt, *Werkst. Korros.*, **22**, 302 (1971).
- 13) P. Markov, C. Roumian, and S. Chorbadev, *Corros. Sci.*, **18**, 103 (1978).
- 14) N. Subramanyan, K. Ramakrishnaiah, S. V. Iyer, and V. Kapali, *Corros. Sci.*, **18**, 1083 (1978).
- 15) B. G. Ateya, B. E. Anadouli, and F. M. A. El-Nizamy, *Bull. Chem. Soc. Jpn.*, **54**, 3157 (1981).
- 16) L. A. Al-Shamma, J. M. Saleh, and N. A. Hikmat, *Corros. Sci.*, **27**, 221 (1987).
- 17) B. E. Conway, "Electrochemical Data," Elsevier, New York (1952), p. 347.
- 18) N. Tanaka and R. Tamamushi, *Electrochim. Acta*, **9**, 953 (1964).
- 19) T. P. Hoar and R. D. Holliday, *J. Appl. Chem.*, **3**, 502 (1953).
- 20) H. Kasseche, "Die Korrosion der Metalle," Springer-



Verlag, Berlin (1966), p. 159.

21) W. J. Larans, F. R. G. Karlaruhe, and F. Mansfeld, Proc. 8th. Inter. Congr. Metal Corrosion, Dechema, West Germany, 6—11, September (1981).

22) G. Trabanelli and V. Carassiti, "Advances in Corrosion Science and Technology," Plenum Press, New York (1950), Vol. 1, p. 147.

23) I. A. Amer and S. A. Darwish, *Corros. Sci.*, **7**, 579 (1967).

24) G. C. Bond, "Catalysis by Metals," Academic Press, New York (1962), pp. 70—71, 126.

25) H. E. Ries, Jr., "Catalysis," ed by P. H. Emmett, Reinhol Publishing Corp. (1954), pp. 6—8.

26) G. Schay, *Acta Chim. Acad. Sci. Hung.*, **3**, 511 (1953).

27) G. C. Bond, "Catalysis by Metals," Academic Press, New York (1962), p. 140.

28) S. A. Isa and J. M. Saleh, *J. Phys. Chem.*, **76**, 2560 (1972).

29) Y. M. Dadiza and J. M. Saleh, *J. Chem. Soc., Faraday Trans. 1*, **68**, 269 (1972).

30) Y. K. Al-Haidari, J. M. Saleh, and M. H. Matloob, *J. Phys. Chem.*, **89**, 3286 (1985).

31) Y. K. Al-Haidari and J. M. Saleh, *J. Chem. Soc., Faraday Trans. 1*, **84**, 3027, 3043 (1988).

32) F. H. Constable, *Proc. R. Soc. London, Ser. A*, **108**, 355 (1952).

33) E. Cremer and G. M. Schwab, *Z. Phys. Chem. (Leipzig)*, **A**, **144**, 243 (1929).

34) E. Cremer, "Advances in Catalysis," Academic Press, New York (1955), Vol. 7, p. 75.

35) C. Kemball, *Proc. R. Soc. London, Ser. A*, **217**, 276 (1953).

36) E. B. Maxted, "Advances in Catalysis," Academic Press, New York (1951), Vol. 3, p. 129.

37) R. H. Griffith and J. D. F. Mrash, "Contact Catalysis," Oxford University Press (1957), pp. 193—207.

---